Density Functional Study on the Mechanism of the C–X (X = Sn, Ge, Si, C, H) σ Bond Oxidative Addition of HC≡CR (R = SnH₃, GeH₃, SiH₃, CH₃, H) to the (PH₃)₂M (M = Ni, Pd, Pt) Complexes. Does the Substrate Approach the Metal in a Parallel or Perpendicular Manner?

Toshiaki Matsubara*,[†,‡] and Kazuyuki Hirao[‡]

Institute for Fundamental Chemistry, 34-4 Takano-Nishihiraki-cho, Sakyo-ku, Kyoto 606-8103, Japan, and Department of Material Chemistry, Graduate School of Engineering, Kyoto University, Sakyo-ku, Kyoto 606-8501, Japan

The activation mechanism of the C–X (X = Sn, Ge, Si, C, H) σ bonds of HC≡CR (R = SnH₃, GeH₃, SiH₃, CH₃, H) is theoretically examined with a density functional method (B3LYP) using the model complexes (PH₃)₂M (M = Ni, Pd, Pt) from the viewpoint of the parallel and perpendicular approach of the incoming substrate. For X = Ge, Si, C, H, the C–X σ bonds approach the Pd parallel to the P–Pd–P plane and are activated in the P–Pd–P plane, as is well-known already for the H–H and C–H bond activation of the H₂ and CH₄ molecules. In contrast, in the case of the highly polarized C–Sn σ bond, the C–Sn σ bond approaches the Pd perpendicularly to the P–Pd–P plane and the activation reaction proceeds by two processes via the resting state **2**, having η²-C–Sn bonding with the Pd. This is obviously different from the conventional σ bond activation in the P–Pd–P plane. The entire potential energy surface for X = Sn was quite smooth, requiring a small energy barrier of only 0.8 kcal/mol due to the attractive interaction of Sn with the Pd at the apical site during the reaction. The difference among the three metals in the same group, Ni, Pd, and Pt, on the C–Sn σ bond activation is also discussed.

1. Introduction

The activation of σ bonds such as H–H, C–H, and C–C, which is an important elementary reaction in organic synthesis, has been studied in great detail from both experimental[1] and theoretical[2] points of view. In the activation of the H–H and C–H bonds of the H₂ and CH₄ molecules on the phosphine-coordinated complexes (PH₃)₂M (M = Pd, Pt), the H–H and C–H axes of the substrate approach the metal parallel to the P–Pd–P plane formed by the bend of the P–Pd–P axis in the initial stage of the reaction.[3,4] This notion is quite

reasonable, because the electron back-donation to the H–H or C–H σ* orbital, which plays a key role in the bond breaking, occurs from the dπ orbital in the P–Pd–P plane enhanced by the electron-donating phosphine ligands:
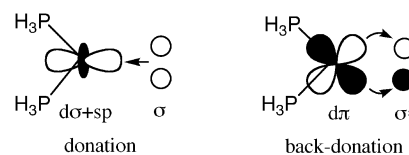
Although it has been thought by theorists that the parallel approach of the σ bond mentioned above is a definite characteristic of σ bond activation on d¹⁰ transition-metal complexes, (PH₃)₂M, transition states which deviate from the square-planar structure have been found in some cases in recent years. Sakaki et al. reported a theoretical result that the C–C or C–Si and P–Pt–P axes largely twist toward each other in the transition state on activation of the C–C and C–Si σ bonds of CH₃CH₃ and CH₃SiH₃ on the (PH₃)₂Pt complex, due to the steric repulsion between the phosphine moiety and the substrate.[5] According to our computations, the transition states for the C–X σ bond activation

† Institute for Fundamental Chemistry.
‡ Kyoto University.
(1) For example, see: (a) Muetterties, E. L.; Rhodin, T. N.; Band, E.; Brucker, C. F.; Pretzer, W. R. *Chem. Rev.* **1979**, *79*, 91. (b) Shilov, A. E. *The Activation of Saturated Hydrocarbons by Transition Metal Complexes*; D. Reidel: Dordrecht, The Netherlands, 1984. (c) Crabtree, R. H. *Chem. Rev.* **1985**, *85*, 245. (d) Cotton, F. A.; Wilkinson, G. In *Advanced Inorganic Chemistry*, 5th ed.; Wiley: New York, 1988. (e) Crabtree, R. H. In *The Organometallic Chemistry of the Transition Metals*, 2nd ed.; Wiley: New York, 1994.
(2) For example, see: (a) Koga, N.; Morokuma, K. *Chem. Rev.* **1991**, *91*, 823. (b) Hay, P. J. In *Transition Metal Hydrides*; Dedieu, A., Ed.; VCH: New York, 1992. (c) Siegbahn, P. E. M.; Blomberg, M. R. A. In *Theoretical Aspects of Homogeneous Catalysis*; van Leeuwen, P. W. N. M., Morokuma, K., van Lenthe, J. H., Eds.; Kluwer Academic Publishers: Dordrecht, The Netherlands, 1995. (d) Musaev, D. G.; Morokuma, K. In *Advances in Chemical Physics*; Prigogine, I., Rice, S. A., Eds.; Wiley: New York, 1996; Vol. XCV.
(3) (a) Low, J. J.; Goddard, W. A., III. *J. Am. Chem. Soc.* **1984**, *106*, 6928. (b) Obara, S.; Kitaura, K.; Morokuma, K. *J. Am. Chem. Soc.* **1984**, *106*, 7482.

(4) (a) Low, J. J.; Goddard, W. A., III. *J. Am. Chem. Soc.* **1984**, *106*, 8321. (b) Low, J. J.; Goddard, W. A., III. *Organometallics* **1986**, *5*, 609. (c) Low, J. J.; Goddard, W. A., III. *J. Am. Chem. Soc.* **1986**, *108*, 6115.

of CH_3XH_3 (X = Sn, Ge, Si, C) deform from the square-planar structure by the mutual twisting of the C−X and P−Pd−P axes even on the $(H_2PC_2H_4PH_2)Pd$ complex with a chelate ligand, which minimizes the steric contact between the phosphine ligands and the substrate.[6]

On the other hand, our density functional study[7] on the [2 + 2 + 1] cycloaddition reaction of two ethynes and one stannylene to form the stannole $(C_4H_4)SnH_2$ catalyzed by the $(PH_3)_2Pd$ complex uncovered a quite interesting subject. The last process is the C−X (X = Sn, C) coupling (which is the reverse of the oxidative addition) to form the stannole. In one of the paths, C−C coupling, the transition state has an exactly square-planar structure; that is, the C−C axis is parallel to the P−Pd−P axis. However, the C−Sn coupling in another path surprisingly showed a unique transition state structure; the C−Sn and P−Pd−P axes are nearly perpendicularly twisted with respect to each other. The same phenomenon was also found in the $(H_2PC_2H_4PH_2)$-Pd complex with the chelate ligand, and this was ascribed to the attractive interaction of the Sn with the Pd at the apical position to stabilize the transition state.[6] Thus, how the incoming substrate approaches the metal, i.e., in a parallel or perpendicular manner

parallel
approach

perpendicular
approach
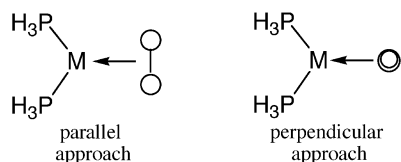
below, is still one of the issues with regard to σ bond activation, although the "parallel approach" has been believed to be the definite answer quite some time.

Therefore, in the present study, we focus on the mechanistic aspects of the C−Sn σ bond activation of $R''C≡CSnR'_3$ (R' = Me, Bu) on phosphine-coordinated d^{10} transition-metal complexes, which is potentially useful as a key step in organic syntheses,[8] and give a theoretical insight from the viewpoint of the parallel and perpendicular approaches of the incoming substrate using the density functional method (B3LYP). We adopted HC≡CR (R = SnH₃, GeH₃, SiH₃, CH₃, H) as the substrate and $(PH_3)_2M$ (M = Ni, Pd, Pt) as the model complexes. Following the explanation of the computational procedures, the C−Sn σ bond activation on the $(PH_3)_2Pd$ complex will first be discussed in the Results and Discussion. The activation of the other C−X (X = Ge, Si, C, H) σ bonds on the $(PH_3)_2Pd$ complex is discussed in the next part, and a comparison among the three metals Ni, Pd, and Pt with regard to C−Sn σ bond activation is then presented. Conclusions are summarized in the last section.

2. Computational Procedures

All calculations were performed using the Gaussian98 program.[9] The calculations of energetics as well as geometry optimizations were carried out at the B3LYP level of theory, which consists of a hybrid Becke + Hartree−Fock exchange and a Lee−Yang−Parr correlation functional with nonlocal corrections.[10] The basis set used, hereinafter referred to as BSI, is the 6-31G** level for the H, C, and Si atoms of HC≡CR (R = SnH₃, GeH₃, SiH₃, CH₃, H), the 6-31G level for the H atom, and the 6-31G* level for the P atom of the spectator ligand PH₃. For Ni, Pd, and Pt, the triple-ζ valence basis functions were augmented by an additional single set of f orbitals with the exponents[11] of 3.130 (Ni), 1.472 (Pd), and 0.993 (Pt) and the effective core potential (ECP) determined by Hay-Wadt[12] to replace the core electrons except for the 18 electrons in the valence shell was used. For Sn and Ge, the (3s,3p)/[2s,2p] basis functions with a polarization function, i.e., 5d with the exponent of 0.183[13] for Sn and 4d with the exponent of 0.246[13] for Ge, and the Hay−Wadt ECP[14] to replace the core electrons, except for the 4 valence electrons, were used.

All equilibrium structures and transition states were optimized without any symmetry restrictions unless otherwise indicated and identified by the number of imaginary frequencies calculated from the analytical Hessian matrix. All the reaction coordinates were followed from the transition state to the reactant and the product by the intrinsic reaction coordinate (IRC) technique.[15] The important structures on the reaction coordinate are arbitrarily selected to determine the reaction processes and are displayed together with the optimized structures in Figure 1. NBO analysis[16] was performed to obtain the atomic orbital (AO) population and the charge. The molecular orbital (MO) energies presented in Table 2 for the $(PH_3)_2M$ (M = Ni, Pd, Pt) complexes were calculated at the Hartree−Fock level. In all the reaction systems, the energies relative to the complexes $(PH_3)_2M$ (**1**; M = Ni, Pd, Pt) and the free HC≡CR (R = SnH₃, GeH₃, SiH₃, CH₃, H) are presented. The binding energy (BE) of the substrate to the metal was calculated as follows: BE = $E[(PH_3)_2M(substrate)]$ − $E[(PH_3)_2M]_{distorted}$ − $E[substrate]_{distorted}$. The stabilization energy is defined as $E[(PH_3)_2M(substrate)]$ − $E[(PH_3)_2M]$ − $E[substrate]$.

3. Results and Discussion

3.1. C−Sn σ Bond Activation on the $(PH_3)_2Pd$ Complex. We first discuss the activation of the C−Sn σ bond of HC≡CSnH₃ on the $(PH_3)_2Pd$ complex, which proceeds by the perpendicular approach unknown so far.

(5) Sakaki, S.; Mizoe, N.; Musashi, Y.; Biswas, B.; Sugimoto, M. *J. Phys. Chem. A* **1998**, *102*, 8027.

(6) Matsubara, T.; Hirao, K. *Organometallics* **2002**, *21*, 2662.

(7) Sahnoun, R.; Matsubara, T.; Yamabe, T. *Organometallics* **2000**, *19*, 5661.

(8) For example, see: (a) Shirakawa, E.; Yoshida, H.; Hiyama, T. *Tetrahedron Lett.* **1997**, *38*, 5177. (b) Shirakawa, E.; Yoshida, H.; Kurahashi, T.; Nakao, Y.; Hiyama, T. *J. Am. Chem. Soc.* **1998**, *120*, 2975. (c) Shirakawa, E.; Hiyama, T. *J. Organomet. Chem.* **1999**, *576*, 169 and references therein.
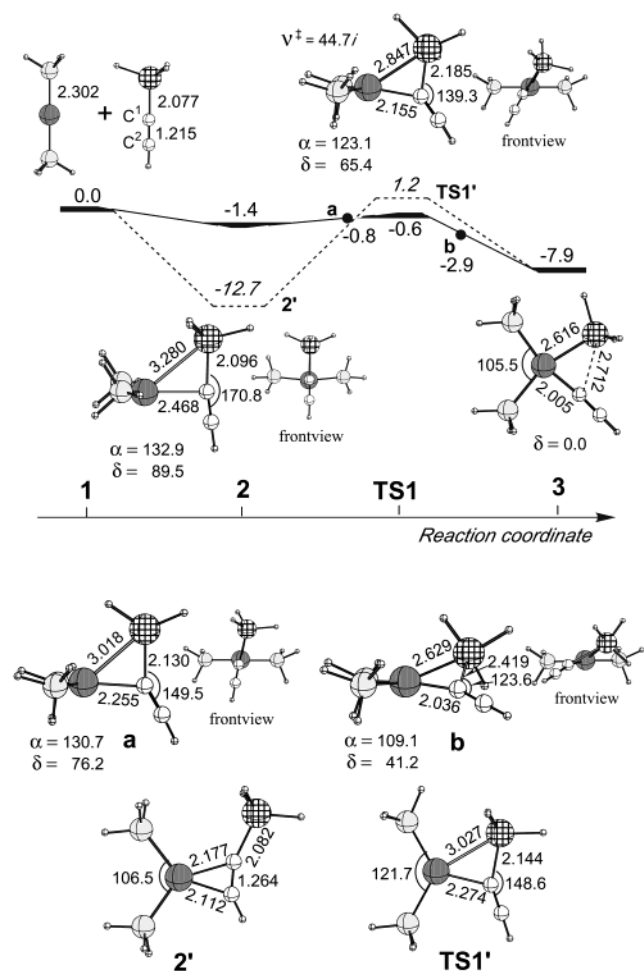
(9) Frisch, M. J.; Trucks, G. W.; Schlegel, H. B.; Scuseria, G. E.; Robb, M. A.; Cheeseman, J. R.; Zakrzewski, V. G.; Montgomery, J. A., Jr.; Stratmann, R. E.; Burant, J. C.; Dapprich, S.; Millam, J. M.; Daniels, A. D.; Kudin, K. N.; Strain, M. C.; Farkas, O.; Tomasi, J.; Barone, V.; Cossi, M.; Cammi, R.; Mennucci, B.; Pomelli, C.; Adamo, C.; Clifford, S.; Ochterski, J.; Petersson, G. A.; Ayala, P. Y.; Cui, Q.; Morokuma, K.; Malick, D. K.; Rabuck, A. D.; Raghavachari, K.; Foresman, J. B.; Cioslowski, J.; Ortiz, J. V.; Stefanov, B. B.; Liu, G.; Liashenko, A.; Piskorz, P.; Komaromi, I.; Gomperts, R.; Martin, R. L.; Fox, D. J.; Keith, T.; Al-Laham, M. A.; Peng, C. Y.; Nanayakkara, A.; Gonzalez, C.; Challacombe, M.; Gill, P. M. W.; Johnson, B. G.; Chen, W.; Wong, M. W.; Andres, J. L.; Head-Gordon, M.; Replogle, E. S.; Pople, J. A. *Gaussian 98*; Gaussian, Inc.: Pittsburgh, PA, 1998.

(10) (a) Lee, C.; Yang, W.; Parr, R. G. *Phys. Rev. B* **1988**, *37*, 785. (b) Becke, D. *J. Chem. Phys.* **1993**, *98*, 5648.

(11) Ehlers, A. W.; Böhme, M.; Dapprich, S.; Gobbi, A.; Höllwarth, A.; Jonas, V.; Köhler, K. F.; Stegmann, R.; Veldkamp, A.; Frenking, G. *Chem. Phys. Lett.* **1993**, *208*, 111.

(12) Hay, P. J.; Wadt, W. R. *J. Chem. Phys.* **1985**, *82*, 299.

(13) Huzinaga, S. *Physical Sciences Data 16, Gaussian Basis Sets for Molecular Calculations*; Elsevier: Amsterdam, 1984.

(14) Wadt, W. R.; Hay, P. J. *J. Chem. Phys.* **1985**, *82*, 284.

(15) Fukui, K.; Kato, S.; Fujimoto, H. *J. Am. Chem. Soc.* **1975**, *97*, 1.

(16) Glendening, E. D.; Reed, A. E.; Carpenter, J. E.; Weinhold F. NBO Version 3.1.

Figure 1. B3LYP/BSI potential energy surface (in kcal/mol) of the oxidative addition of the C−Sn σ bond of HC≡CSnH$_3$ to the (PH$_3$)$_2$Pd complex **1**, together with the optimized structures (in Å and deg) of the reactant **1** with the free HC≡CSnH$_3$, the intermediate **2**, the transition state **TS1**, and the product **3** at the B3LYP/BSI level. The structures at points a and b on the reaction coordinate are also displayed. The imaginary frequency (cm^{-1}) is shown for the transition state **TS1**. α and δ represent the angle ∠P−Pd−P and the dihedral angle ∠P−m-Pd−Sn (m is the midpoint between two P atoms), respectively. The dihedral angle δ was artificially fixed to zero during the reaction **1** → **2′** → **TS1′** →**3** , the potential energy surface of which is shown by the dashed line.

The reaction consists of two processes, which is divided by the resting state **2**, as shown in Figure 1. In the first process, the incoming HC≡CSnH$_3$ coordinates to the Pd to form the intermediate **2**, in which the C^1−Sn axis interacts with the Pd by the η^2 mode. It should be noted here that the C^1−Sn axis is not parallel but perpendicular to the P−Pd−P axis, although the C^1−Sn axis only slightly deviates from 90°, by 0.5° to be exact. Another characteristic of the structural features is that C^1 is just at the equatorial position and Sn occupies the apical position. The P−Pd−P axis bends back with a ∠P−Pd−P angle of 132.9°. The unoccupied sp-hybridized orbital of the Pd in the P−Pd−P plane is thereby stabilized, while the occupied dπ orbital of the Pd in the P−Pd−P plane is destabilized in energy by the electronic effect of the electron-donating phosphine ligands[17] to interact with the C−Sn σ bond by the well-known electron donation and back-donation in the P−Pd−P

Table 1. NBO Analysis of Free HC≡CR (R = SnH$_3$, GeH$_3$, SiH$_3$, CH$_3$, H)

R	C^1−X σ bond % X	C^1−C^2 σ bond % C^1	C^1−C^2 π bond % C^1	atomic charge		
				X	C^1	C^2
SnH$_3$	24.5	49.1	51.4	1.2698	−0.5348	−0.2021
GeH$_3$	27.3	49.7	51.6	0.9939	−0.5030	−0.1849
SiH$_3$	28.0	49.9	52.0	0.9025	−0.5046	−0.1630
CH$_3$	50.1	50.8	49.5	−0.7537	−0.0199	−0.2552
H	37.8	50.0	50.0	0.2438	−0.2438	−0.2438

plane. Nevertheless, why is the C−Sn σ bond not parallel but perpendicular to the P−Pd−P plane in the intermediate **2**? We have determined that it is because the perpendicular approach stabilizes the transition state in energy and makes the potential energy surface smooth, as described below.

As shown in Table 1, the C−Sn σ bond is largely polarized and the electron is accumulated at the C^1 atom so that the C≡C π orbital of C^1 directed toward Pd interacts with the valence sp-hybridized orbital of Pd in the P−Pd−P plane by its electron donation, with a Pd−C^1 distance of 2.468 Å. Also, we should not forget that the Pd sp-hybridized orbital is stabilized by the bending of the P−Pd−P axis to make this interaction facile, as mentioned above. Here, the π orbital of C^1 is considered to play a key role in the perpendicular interaction in **2**, because a similar perpendicular interaction could not be found for CH$_3$SnH$_3$ without the π orbital.[6] The electron donation through C^1 furthermore

donation   back-donation
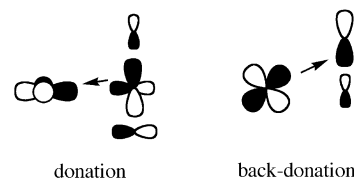
promotes the polarization of the C−Sn bond and enhances the electron deficiency at Sn. On the other hand, another C^2 π orbital directed toward the Pd must avoid repulsive contact with the occupied Pd dπ orbital. When the C^1−Sn axis is parallel to the P−Pd−P plane, the repulsive interaction with the Pd dπ orbital in the P−Pd−P plane enhanced by the electron-donating phosphine ligands reaches a maximum. In contrast, when the C^1−Sn axis is perpendicular to the P−Pd−P plane, the repulsive interaction with the Pd dπ is at a minimum, as shown by the small deformation of the HC≡CSnH$_3$ substrate by the bending of the Sn−C^1−C^2 axis with an ∠Sn−C^1−C^2 angle of 170.8°, because the Pd dπ orbital perpendicular to the P−Pd−P plane is not enhanced. Therefore, the electron-deficient Sn atom interacts with the Pd by electron back-donation from the occupied dπ orbital of the Pd perpendicular to the P−Pd−P plane and occupies an apical position. As a result of both the electron donation and the back-

(17) (a) Saillard, J.-Y.; Hoffmann, R. *J. Am. Chem. Soc.* **1984**, *106*, 2006. (b) Albright, T. A.; Burdett, J. K.; Whangbo, M. H. In *Orbital Interactions in Chemistry*, Wiley: New York, 1985. Also, see Table 2; the energy level of the sp$_x$-hybridized orbital is lowered, and in contrast, that of the d$_{xy}$ orbital is raised, with the decrease in the ∠P−M−P angle β.
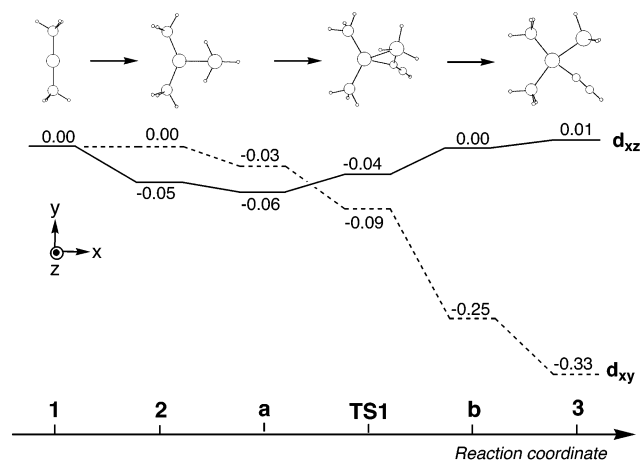
Figure 2. Changes in the population of the Pd d_{xz} (solid line) and d_{xy} (dashed line) orbitals during the oxidative addition of the C–Sn σ bond of HC≡CSnH₃ to the (PH₃)₂-Pd complex **1**. The negative and the positive signs of the values represent decreases and increases in population, respectively.

donation interactions (see the orbital illustration presented above), the C–Sn bond is stretched to 2.096 Å. The binding energy of the HC≡CSnH₃ substrate to the Pd in **2** was calculated to be 10.5 kcal/mol. The small stabilization energy of **2** (1.4 kcal/mol; see below) is ascribed to structural deformation due to the bending of the P–Pd–P axis.

In the second process after the perpendicular approach of the C–Sn σ bond to the Pd, the HC≡CSnH₃ substrate starts to rotate around the Pd–C¹ axis. A decrease in the $\angle$Sn–C¹–C² angle, which reduces electronic repulsion between the C² π orbital and the Pd $d\pi$ orbital in the P–Pd–P plane mentioned earlier, would induce this rotation of the substrate. With the intermediate **2** as a starting point, both Pd–Sn and Pd–C¹ distances are shortened as the C¹–Sn axis rotates, and the C¹–Sn distance is elongated with a decrease in the $\angle$P–Pd–P angle. The C¹–Sn bond breaking is finally completed by the strong electron back-donation from the destabilized $d\pi$ orbital of the Pd in the P–Pd–P plane to the C¹–Sn σ^* orbital, in which the Pd becomes divalent. The transition state **TS1** is relatively early, as shown by the small rotation of the substrate HC≡CSnH₃ by about 24° and the stretch of the C¹–Sn bond proceeding by only 17%. The Sn atom completely moves into the P–Pd–P plane in the product **3**, which has a square-planar structure.

We followed the amount of electron flow from the Pd $d\pi$ orbital to the C¹–Sn σ^* orbital by the electron back-donation during the activation reaction. As shown in Figure 2, electron back-donation occurs only from the Pd d_{xz} orbital perpendicular to the P–Pd–P plane at the intermediate **2**, and it becomes maximum at point a on the reaction coordinate, in which the C¹–Sn bond comes closest to the Pd atom in the perpendicular approach. After passing through point a, the electron back-donation from the Pd d_{xy} orbital in the P–Pd–P plane to the C¹–Sn σ^* orbital gradually increases as the rotation of the C¹–Sn axis proceeds.

Since the attractive interaction of the Sn with the Pd d_{xz} orbital perpendicular to the P–Pd–P plane by the electron back-donation on the way from the intermedi-

ate **2** to the product **3** energetically stabilizes the potential energy surface and significantly lowers the transition state **TS1** in energy, the potential energy surface is quite smooth, with a small energy barrier of less than 1 kcal/mol (Figure 1). The intermediate **2** is stabilized by 1.4 kcal/mol compared to the reactant **1**. The transition state **TS1** is also 0.6 kcal/mol more stable in energy than the reactant **1**, and the reaction is 7.9 kcal/mol exothermic. However, if the reaction sphere is artificially restricted to the P–Pd–P plane without the contribution of the Pd $d\pi$ orbital perpendicular to the P–Pd–P plane, the energy of the transition state **TS1′** rises by 1.8 kcal/mol and becomes higher than that of **1** (Figure 1). An additional imaginary frequency for the rotation of the bound HC≡CSnH₃ around the Pd–C¹ axis revealed that **TS1′** is not the true transition state. The Pd–Sn and Pd–C¹ distances are longer and the C¹–Sn distance is shorter for **TS1′** than for **TS1**, because the electronic repulsion between the C² π orbital and the Pd $d\pi$ orbital in the P–Pd–P plane enhanced by the electron-donating phosphine ligands appears while the contribution of the Pd $d\pi$ orbital perpendicular to the P–Pd–P plane to the attractive interaction of the Sn with the Pd disappears in **TS1′**. The transition state **TS1′** was connected to **3** on the product side and not to the η^2-C–Sn π-complex but to the η^2-C≡C π-complex **2′** on the reactant side by the IRC calculation, although this reaction pathway passing through the false transition state **TS1′** actually does not exist. Thus, the unique η^2-C–Sn π interaction is possible only in the perpendicular plane. It should be noted here that the Pd–C¹ distance is longer by 0.065 Å than the Pd–C² distance in **2′** due to the electronic effect of the SnH₃ substituent; the accumulated electron at the C¹ by the strong polarization of the C¹–Sn σ bond mentioned earlier (see Table 1) weakens the electron back-donation from the Pd $d\pi$ orbital in the P–Pd–P plane to the π^* orbital of C¹.

3.2. C–Ge, C–Si, C–C, and C–H σ Bond Activation on the (PH₃)₂Pd Complex. When the Sn atom is replaced by the other atoms in the same group, the intermediate corresponding to **2** found for Sn does not exist. This fact can be ascribed to the polarization of the C–X bond, which is weaker for Ge, Si, and C than for Sn (see Table 1). In addition, the C–X σ^* orbital is also higher in energy for Ge, Si, and C than for Sn.[18] Therefore, C–X σ bonds other than the C–Sn σ bond cannot interact with the Pd $d\pi$ orbital perpendicular to the P–Pd–P plane. In the case of X = Ge, Si, the η^2-C≡C π-complexes **4** and **6** were the intermediates, respectively, as presented in Figure 3. The interaction by electron donation from the C≡C π orbital to the Pd sp-hybridized orbital and back-donation from the Pd $d\pi$ orbital to the C≡C π^* orbital in the P–Pd–P plane in the π complexes **4** and **6**, which is known as the Dewar–Chatt–Duncanson model,[19] is broken to reach the transition states **TS2** and **TS3**. The analysis of the atomic orbital (AO) population of the Pd d orbitals showed that the Pd $d\pi$ orbital perpendicular to the

(18) The sequence in the energy level (in hartree) of the σ and σ^* orbitals of the C–X (X = Sn, Ge, Si, C, H) σ bonds of HC≡CR (R=SnH₃, GeH₃, SiH₃, CH₃, H) was as follows: for σ, Sn (−0.5007) > Ge (−0.5306) > Si (−0.5839) > H (−0.5934) > C (−0.6765); for σ^*, H (0.5001) > C (0.4741) > Ge (0.3009) > Si (0.2544) > Sn (0.1843).
(19) (a) Dewar, M. J. S. *Bull. Soc. Chim. Fr.* **1951**, C71. (b) Chatt, J.; Duncanson, L. A. *J. Chem. Soc.* **1953**, 2939.
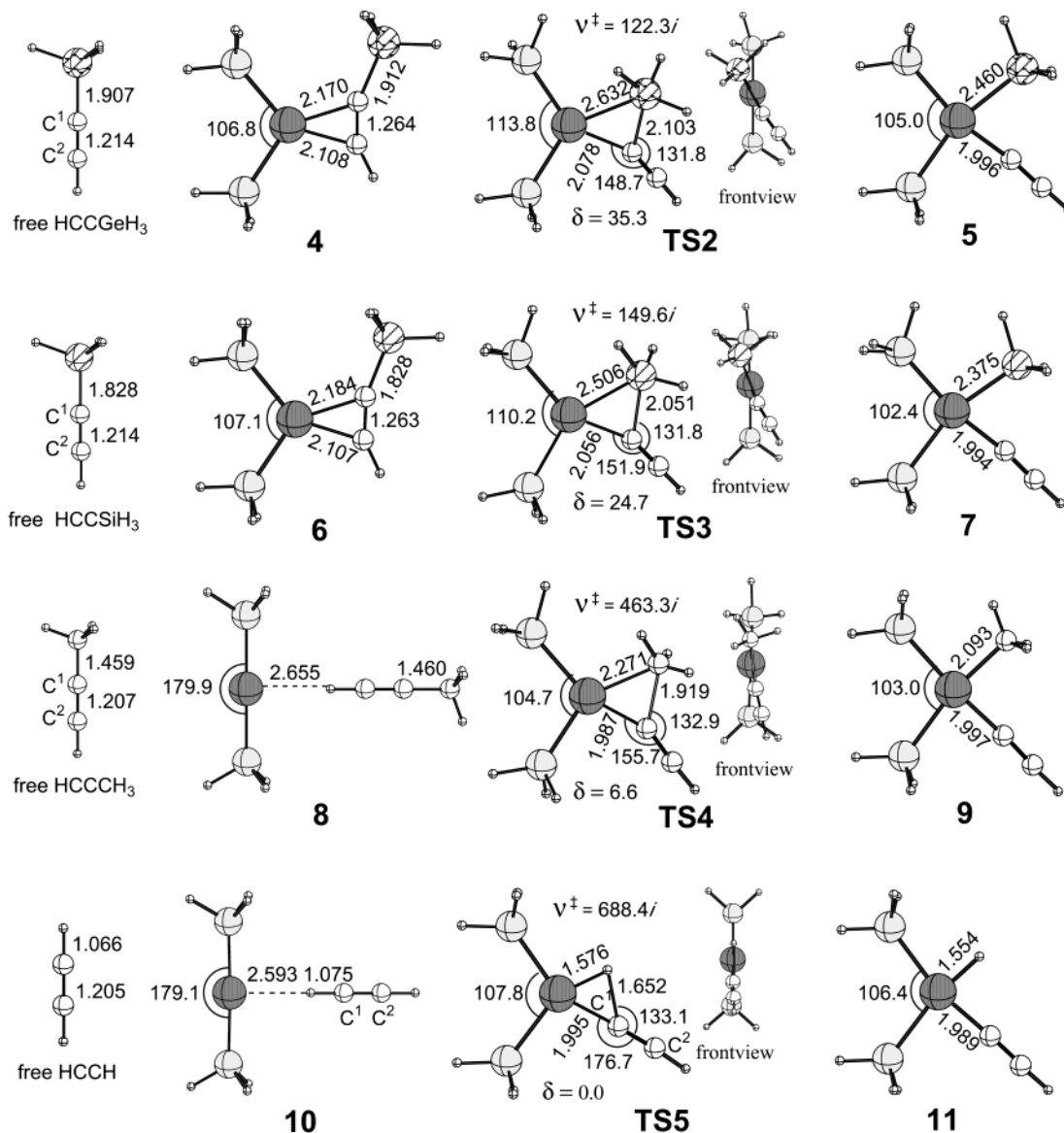
Figure 3. B3LYP/BSI-optimized structures (in Å and deg) of the intermediates (**4**, **6**, **8**, **10**), the transition states (**TS2**, **TS3**, **TS4**, **TS5**), and the products (**5**, **7**, **9**, **11**) for the oxidative addition of the C−X (X = Ge, Si, C, H) σ bonds of HC≡CR (R = GeH$_3$, SiH$_3$, CH$_3$, H) to the (PH$_3$)$_2$Pd complex **1**, together with those of free HC≡CR. δ represents the dihedral angle ∠P−m-Pd−X (m is the midpoint between two P atoms). The imaginary frequencies (cm^{-1}) are shown for the transition states.

P−Pd−P plane does not participate in the activation reaction and the C−X σ bonds are activated in the P−Pd−P plane by conventional electron donation from the C−X σ orbital to the Pd sp orbital and back-donation from the Pd dπ orbital in the P−Pd−P plane to the C−X σ* orbital. Nevertheless, the Pd−X−C^1 plane deviates from the P−Pd−P plane, i.e., two planes mutually twist, in the transition state to avoid the electronic repulsion between the C≡C π orbital and the Pd dπ orbital in the P−Pd−P plane enhanced by the electronic effect of the phosphine ligands and the steric contact between the XH$_3$ and the PH$_3$ ligand in the vicinity of XH$_3$.

On the other hand, for X = C, H, the alkyne H coordinates to Pd by a weak electrostatic interaction in the intermediates **8** and **10**, in which the P−Pd−P axis is almost linear.[20] For X = H, the coordinated alkyne slightly shifts in the P−Pd−P plane, breaking the weak electrostatic interaction, and the nearby C−H σ bond approaches the Pd precisely parallel to the P−Pd−P

plane in the conventional manner, as is already well-known for the H−H and C−H bond activation of the H$_2$ and CH$_4$ molecules. Therefore, the transition state **TS5** for X = H is square planar, although the transition state **TS4** for X = C is slightly twisted. Also for X = C, H, the activation takes place in the P−Pd−P plane without the support of the Pd dπ orbital perpendicular to the P−Pd−P plane. As one can see in Figure 3, the twist angle gradually decreases in the order Ge (35.3°) > Si (24.7°) > C (6.6°) and becomes zero for H. This trend in the twist angle can be reasonably understood by a repulsive contact between the C≡C π orbital and

---

(20) In the case of X = C, H, the transition states **TS4** and **TS5** were connected to the intermediates **8** and **10**, respectively, on the reactant side by the IRC calculations, because the C^1 goes away from the Pd. However, in the case of X = Ge, Si, the C^1 stays around the Pd during the reaction by its electron donation due to the stronger polarization of the X−C^1 bond, where the electron is accumulated on C^1. Therefore, the transition states were connected to the corresponding π complexes.
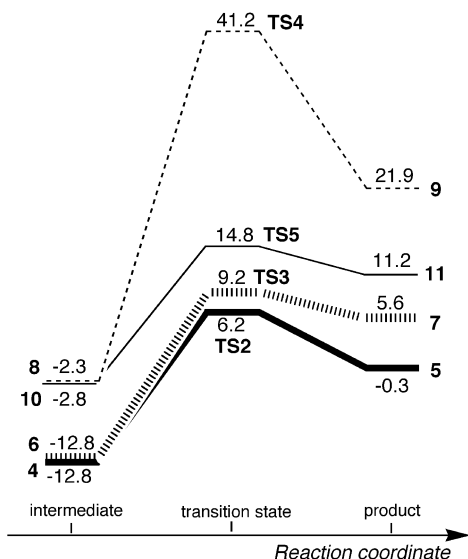
Figure 4. B3LYP/BSI potential energy surfaces (in kcal/mol) of the oxidative addition of the C−X (X = Ge, Si, C, H) σ bonds of HC≡CR (R=GeH₃, SiH₃, CH₃, H) to the (PH₃)₂Pd complex **1**. The energies relative to **1** and the free HC≡CR are presented. The boldface, vertically dashed, solid, and horizontally dashed lines are for X = Ge, Si, H, C, respectively.
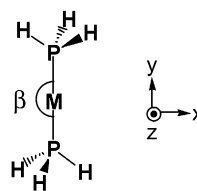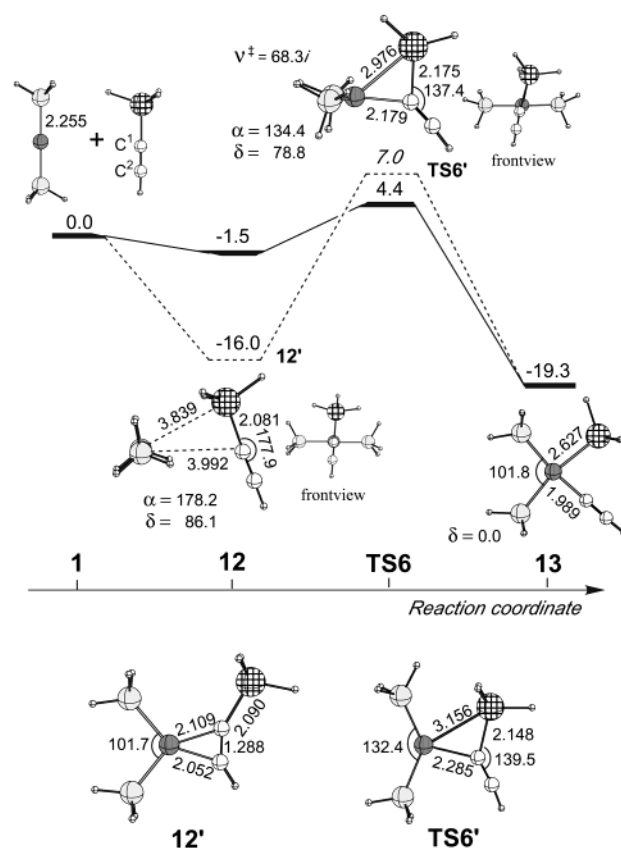

Figure 5. B3LYP/BSI potential energy surface (in kcal/mol) of the oxidative addition of the C−Sn σ bond of HC≡CSnH₃ to the (PH₃)₂Pt complex **1**, together with the optimized structures (in Å and deg) of the reactant **1** with the free HC≡CSnH₃, the intermediate **12**, the transition state **TS6**, and the product **13** at the B3LYP/BSI level. The imaginary frequency (cm⁻¹) is shown for the transition state **TS6**. α and δ represent the angle ∠P−Pt−P and the dihedral angle ∠P−m-Pt−Sn (m is the midpoint between two P atoms), respectively. The dihedral angle δ was artificially fixed to zero during the reaction **1** → **12′** → **TS6′** → **13**, the potential energy surface of which is shown by the dashed line.

the Pd dπ orbital enhanced in the P−Pd−P plane, which increases in the order Ge > Si > C > H, since the steric stress which comes from the XH₃ moiety in the transition state is reflected in the ∠Pd−C¹−C² angle decreasing in the order H > C > Si > Ge, according to the size of the XH₃ moiety. The ∠X−C¹−C² angle of 132−133° was nearly the same among X = Ge, Si, C, H.

The potential energy surfaces of the C−X σ bond activation for X = Ge, Si, C, H are presented together in Figure 4. Although the reaction starting from **1** is almost neutral for Ge, it is endothermic for the others. The transition state is higher in energy than the reactant **1** for all the cases of X = Ge, Si, C, H, in contrast to the case for X = Sn, with the support of the Pd dπ orbital perpendicular to the P−Pd−P plane, its energy becoming higher in the order C > H > Si > Ge. The entire potential energy surface is shifted down, and the endothermicity decreases in the sequence C > H > Si > Ge. One can easily notice a tendency that the energy barrier from the intermediate to the transition state decreases with a decrease in endothermicity, although the energy barrier for Ge and Si from the stable π-complex to the transition state is larger than that for H from the much less stable intermediate **10** to the transition state **TS5**.

3.3. C−Sn σ Bond Activation on the (PH₃)₂Pt and (PH₃)₂Ni Complexes. Even for the (PH₃)₂Pt complex, the activation mechanism of the C−Sn σ bond of HC≡CSnH₃ did not change. The substrate HC≡CSnH₃ approaches the Pt perpendicularly to the P−Pt−P plane to form the intermediate **12**, as presented in Figure 5. After passing through the resting state **12**, the C−Sn σ bond is broken, with the rotation of HC≡CSnH₃ induced by a decrease in the ∠Sn−C¹−C² angle. The structure of the intermediate **12** deviates slightly from C_s symmetry with a small rotation of the bound HC≡CSnH₃ around the Pt−C¹ axis by about 4°. The Pt−Sn and Pt−C¹ distances are quite long compared to the case for

Pd, and both Sn−C¹−C² and P−Pt−P axes are nearly linear. However, the C¹ and Sn atoms occupy the equatorial and apical positions, respectively, which is similar to the case for Pd. The binding energy of HC≡CSnH₃ in the intermediate **12** was calculated to be only 1.7 kcal/mol, which is much smaller than that for Pd (10.5 kcal/mol). These differences of Pt from Pd can be understood by the difficulty of bending the P−Pt−P axis, as shown by the change in the total energy of the (PH₃)₂M complexes with a decrease in the angle β (Table 2), since there is not a crucial difference between Pd and Pt with regard to the energy levels of the sp-hybridized orbital and the dπ (d_{xz}) orbital perpendicular to the P−M−P plane (for example, see the case of β = 120° in Table 2). In the transition state **TS6**, both Pt−Sn and Pt−C¹ distances are significantly shortened, with a decrease in the angles ∠P−Pt−P and ∠Sn−C¹−C², but the Pt−Sn−C¹ plane inclines by only 11° from the perpendicular due to the early transition state.

The transition state **TS6** is less stable in energy than the reactant **1** despite the large exothermicity of 19.3 kcal/mol, and an energy barrier of 5.9 kcal/mol, which

Table 2. Molecular Orbital (MO) Energies (in hartree) of the sp-Hybridized and d Orbitals of the Metals of the (PH$_3$)$_2$M (M = Ni, Pd, Pt) Complexes at the Hartree−Fock Level and the Relative Total Enegies (kcal/mol) at the B3LYP Level[a]

β	sp$_x$	d$_{xz}$	d$_{xy}$	rel total energy
180	0.0719	−0.3259	−0.3168	0.0
	0.0812	**−0.3359**	**−0.3453**	**0.0**
	0.0692	*−0.3194*	*−0.3443*	*0.0*
150	0.0608	−0.3230	−0.2982	1.4
	0.0649	**−0.3392**	**−0.3161**	**2.0**
	0.0661	*−0.3265*	*−0.3107*	*4.4*
120	0.0575	−0.3198	−0.2677	7.5
	0.0616	**−0.3461**	**−0.2765**	**9.4**
	0.0597	*−0.3412*	*−0.2645*	*18.1*

[a] Numbers in Roman, boldface, and italic type are for Ni, Pd, and Pt, respectively. β values are given in deg.

is larger than that for Pd, is required. When the activation reaction is artificially forced to take place in the P−Pt−P plane with the assumption of the parallel approach, the transition state **TS6′**, which is not the true transition state, having two imaginary frequencies, was shifted up by 2.6 kcal/mol, indicating that the perpendicular approach is energetically more favorable than the parallel approach, which is similar to the case for Pd. The transition state **TS6′** was connected to not the η^2-C−Sn π-complex but the η^2-C≡C π-complex **12′** on the reactant side. It should be noted here that the activation reaction is more advanced in **TS6** than in **TS6′** despite the early transition state, as shown by the shorter Pt−Sn and Pt−C^1 distances and the longer C^1−Sn distance in **TS6** as compared to **TS6′**.

In the case of Ni, **TS7** is not the resting state but the transition state between the products **14** for the switch of the positions between the SnH$_3$ and C≡CH ligands, as presented in Figure 6. The Sn−C^1 axis of HC≡CSnH$_3$ is exactly perpendicular to the P−Ni−P plane in **TS7**, as shown by $\delta = 90°$, the structure having C_s symmetry. The Ni−Sn and Ni−C^1 distances are significantly shortened to 2.552 and 1.869 Å, respectively, which are only 0.004−0.033 Å longer than those in the product **14**. On the other hand, the Sn−C^1 bond is stretched to 2.289 Å, and the angles ∠Sn−C^1−C^2 and ∠P−Ni−P are reduced to 123.6 and 119.8°, respectively. These structural features of **TS7**, which are different from those of the corresponding **2** for Pd, would originate from the dπ (d$_{xz}$) orbital of the Ni perpendicular to the P−Ni−P plane, which is much higher in energy compared to that of Pd (see the case of $\beta = 120°$ in Table 2) and makes the electron back-donation to the Sn facile to strengthen the interaction with Sn. Thus, the electron-deficient Sn is more strongly attracted at the apical site and the transition state **TS7** is much more stabilized in energy than the reactant **1**. Indeed, the binding energy of HC≡CSnH$_3$ in **TS7** was quite large (46.3 kcal/mol).

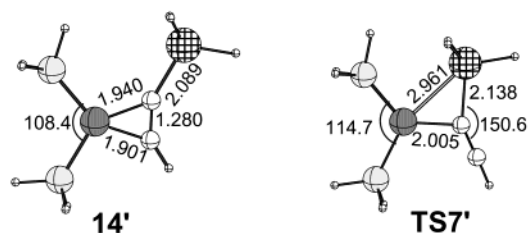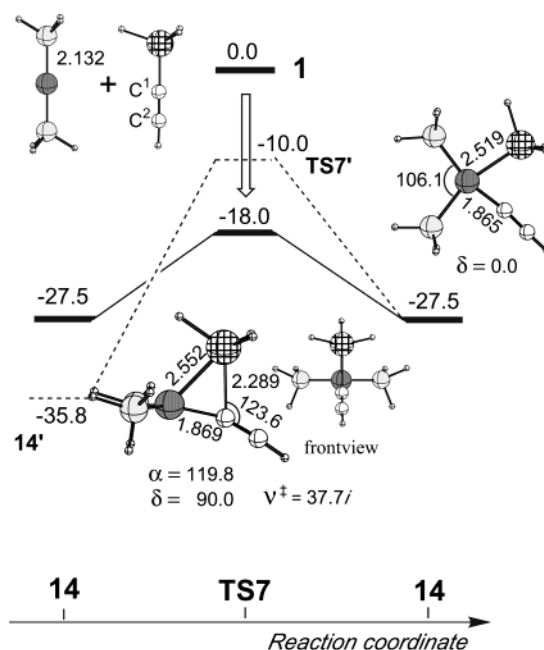As displayed in Figure 6, the reaction starting from **1** proceeds by the perpendicular approach of

Figure 6. B3LYP/BSI potential energy surface (in kcal/mol) of the oxidative addition of the C−Sn σ bond of HC≡CSnH$_3$ to the (PH$_3$)$_2$Ni complex **1**, together with the optimized structures (in Å and deg) of the reactant **1** with the free HC≡CSnH$_3$, the transition state **TS7**, and the product **14** at the B3LYP/BSI level. The imaginary frequency (cm^{-1}) is shown for the transition state **TS7**. α and δ represent the angle ∠P−Ni−P and the dihedral angle ∠P−m−Ni−Sn (m is the midpoint between two P atoms), respectively. The dihedral angle δ was artificially fixed to zero during the reaction **14′** → **TS7′** → **14**, the potential energy surface of which is shown by the dashed line.

HC≡CSnH$_3$ to the Ni of the (PH$_3$)$_2$Ni complex, and the sufficiently preactivated C−Sn σ bond in the plane perpendicular to the P−Ni−P plane by the strong electron back-donation from the Ni d$_{xz}$ orbital is readily broken in the P−Ni−P plane by the electron back-donation from the d$_{xy}$ orbital without an energy barrier. The HC≡CSnH$_3$-bound complex that is formed, **TS7**, decreases energetically to the product **14** along the potential energy surface with the rotation of the C^1−Sn axis. The transition state **TS7′** artificially confined in the P−Ni−P plane was less stable in energy by 8 kcal/mol than **TS7** and was a false transition state with three imaginary frequencies, which was connected to the η^2-C≡C π-complex **14′** and the product **14**.

4. Concluding Remarks

We ahve focused on the mechanistic aspects of the activation of C−X (X = Sn, Ge, Si, C, H) σ bonds on phosphine-coordinated d^{10} transition-metal complexes and gave a theoretical insight from the viewpoint of the

parallel and perpendicular approach of the substrate with the density functional method (B3LYP) using the model system HC≡CR (R = SnH_3, GeH_3, SiH_3, CH_3, H) + $(PH_3)_2M$ (M = Ni, Pd, Pt). As is well-known for the H—H and C—H bond activation of the H_2 and CH_4 molecules, the C—H σ bond of ethyne for X = H approaches the Pd parallel to the P—Pd—P plane and is activated in the P—Pd—P plane. However, in contrast to this, it was found that the C—Sn σ bond of HC≡CSnH₃, which is highly polarized, approaches the Pd perpendicularly to the P—Pd—P plane and the activation proceeds by two processes via the resting state **2**. This is obviously different from the conventional σ bond activation in the P—Pd—P plane. The η^2-C—Sn π-complex **2** formed in the first stage has the C—Sn axis perpendicular to the P—Pd—P plane, in which the C and Sn atoms occupy the equatorial and the apical positions, respectively, due to electron donation from the electron-rich C to the Pd sp-hybridized orbital through the C π orbital directed toward the Pd and electron back-donation from the Pd $d\pi$ orbital perpendicular to the P—Pd—P plane to the electron-deficient Sn. The preactivated C—Sn σ bond in the first stage rotates around the Pd—C axis in the second stage, and the C—Sn bond breaking is completed by the electron back-donation from the Pd $d\pi$ orbital in the P—Pd—P plane enhanced by the electron-donating phosphine ligands to the C—Sn σ^* orbital. The entire potential energy surface is quite smooth, requiring a small energy barrier of only 0.8 kcal/mol, because the attractive interaction of the Sn with the Pd at the apical site during the rotation of the C—Sn axis significantly stabilizes the potential energy surface and lowers the transition state in energy. On the other hand, the activation of less polarized C—X (X = Ge, Si, C, H) σ bonds takes place in the P—Pd—P plane by a parallel approach without the support of the Pd $d\pi$ orbital perpendicular to the P—Pd—P plane, through conventional electron donation from the C—X σ orbital to the Pd sp-hybridized orbital and back-donation from the Pd $d\pi$ orbital in the P—Pd—P plane to the C—X σ^* orbital. However, the C—X σ bond deviates from the P—Pd—P plane in the transition state to avoid repulsive contact between the C≡C π orbital and the enhanced Pd $d\pi$ orbital in the P—Pd—P plane, except for X = H, in which this repulsive interaction is minimized due to the small size of H. The activation of the C—Sn σ bond similarly proceeds by the perpendicular approach also for Ni and Pt, although the reaction is downhill for Ni and requires a large energy barrier of 5.9 kcal/mol for Pt.

Supporting Information Available: Listings giving the optimized Cartesian coordinates of all equilibrium structures and transition states presented in this paper. This material is available free of charge via the Internet at http://pubs.acs.org.

OM020208O